AIP | Journal of Applied Physics

Size effects of primary/secondary twins on the atomistic deformation mechanisms in hierarchically nanotwinned metals

Fuping Yuan and Xiaolei Wu

Citation: J. Appl. Phys. **113**, 203516 (2013); doi: 10.1063/1.4808096
View online: http://dx.doi.org/10.1063/1.4808096
View Table of Contents: http://jap.aip.org/resource/1/JAPIAU/v113/i20
Published by the AIP Publishing LLC.

Additional information on J. Appl. Phys.

Journal Homepage: http://jap.aip.org/
Journal Information: http://jap.aip.org/about/about_the_journal
Top downloads: http://jap.aip.org/features/most_downloaded
Information for Authors: http://jap.aip.org/authors

ADVERTISEMENT

Downloaded 13 Jun 2013 to 159.226.199.8. This article is copyrighted as indicated in the abstract. Reuse of AIP content is subject to the terms at: http://jap.aip.org/about/rights_and_permissions

JOURNAL OF APPLIED PHYSICS **113**, 203516 (2013)

Size effects of primary/secondary twins on the atomistic deformation mechanisms in hierarchically nanotwinned metals

Fuping Yuan[a] and Xiaolei Wu
State Key Laboratory of Nonlinear Mechanics, Institute of Mechanics, Chinese Academy of Science, Beijing 100190, People's Republic of China

(Received 25 March 2013; accepted 14 May 2013; published online 29 May 2013)

A series of large-scale molecular dynamics simulations have been performed to investigate the tensile properties of nanotwinned (NT) copper with hierarchically twinned structures (HTS). For the same grain size d and the same spacing of primary twins λ_1, the average flow stress first increases as the spacing of secondary twins λ_2 decreases, reaching a maximum at a critical λ_2, and then decreases as λ_2 becomes even smaller. The smaller the spacing for λ_1, the smaller the critical spacing for λ_2. There exists a transition in dominating deformation mechanisms, occurring at a critical spacing of λ_2 for which strength is maximized. Above the critical spacing of λ_2, the deformation mechanisms are dominated by the two Hall-Petch type strengthening mechanisms: (a) partial dislocations emitted from grain boundaries (GBs) travel across other GBs and twin boundaries (TBs); (b) partial dislocations emitted from TBs travel across other TBs. Below the critical spacing of λ_2, the deformation mechanism is dominated by the two softening mechanisms: (a) Partial dislocations emitted from boundaries of the primary twins travel parallel to the TBs of the secondary twins, leading to detwinning of the secondary twins; (b) Boundaries of the primary twins shift entirely, leading to thickening in one part of primary twins and thinning in the other part of primary twins. The present results should provide insights to design the microstructures for reinforcing the mechanical properties in the NT metals with HTS. © *2013 AIP Publishing LLC*. [http://dx.doi.org/10.1063/1.4808096]

I. INTRODUCTION

Stronger metals and alloys are always desirable for structural applications in modern industry. Such expectation has been realized through the emergence of several strategies in recent decades, such as, grain size refinement, solid solution alloying, and precipitating strengthening.[1,2] More recently, engineering coherent twin boundaries (TBs) at the nanoscale have been regarded as an efficient way to achieve high strength while maintaining substantial ductility.[3–5] Moreover, the maximum strength could be realized at a critical twin spacing in such ultrafine-grained Cu with nanoscale growth twins, generally with thin film samples synthesized using the pulsed electro-deposition technique. Molecular dynamics (MD) simulations[6–8] have shown that there exists a transition in deformation mechanisms at the critical twin spacing, i.e., from the classical Hall-Petch type strengthening due to dislocation pile-up at twin planes to a dislocation-nucleation-controlled softening mechanism with twin-boundary migration. It was also found that the critical twin spacing is proportional to the grain size through both MD simulations and theoretical models.[6,9,10]

Severe plastic deformation (SPD) techniques, such as cold rolling,[11,12] equal channel angular pressing,[13,14] and high-pressure torsion (HPT),[15] have been now widely used for processing of bulk ultrafine-grained materials from coarse-grained structures. In those methods, the mechanism governing deformation-induced grain refinement is found to be dominated by dislocation activities, when deformed at quasi-static strain rates ($<10^0\,s^{-1}$) and at ambient temperature. However, deformation twinning is another important deformation mechanism for grain refinement in some metals and alloys with low stacking fault energies (SFEs), especially with deformation conditions at high strain rates and low temperatures. Experimentally, the hierarchically twinned structures (HTS) could be achieved in these materials, as evidenced in the samples processed with the newly developed techniques at high strain rates and/or low temperatures, such as dynamic plastic deformation (DPD),[16,17] surface mechanical attrition treatment (SMAT),[18,19] and surface mechanical grinding treatment (SMGT).[20] For example, the secondary twins could be generated in the primary twins in the twinning induced plasticity (TWIP) steels[21] and 304 stainless steels[22] during the process of SMAT, and the tertiary twins appear in the secondary twins during the subsequent tensile testing. Experiments have also shown that high rate and low temperature deformation may lead to formation of secondary twins inside primary twin/matrix lamellae in those fcc metals with medium SFEs such as Cu and Ni.[22,23] As classified by the sources of the twinning partials, three types of twinning mechanisms for nanostructured multiple twins have been proposed: (1) Twinning partials from different grain boundaries (GBs) meet each other in a confined area inside grain;[23,24] (2) Self partial-multiplication twinning mechanism;[23,25,26] (3) Rebound mechanism.[27,28] Recent experiments and theoretical model have also shown that the hierarchically twinned structures with the secondary twins at

[a]Author to whom correspondence should be addressed. Electronic mail: fpyuan@lnm.imech.ac.cn

 © 2013 AIP Publishing LLC

Downloaded 13 Jun 2013 to 159.226.199.8. This article is copyrighted as indicated in the abstract. Reuse of AIP content is subject to the terms at: http://jap.aip.org/about/rights_and_permissions

the nanoscale can be a novel nanostructured design to achieve higher strength.[21,29]

For the mechanical properties of the nanotwinned metals with HTS, a few efforts[21,29] have been carried out to investigate the twin spacing effects of primary/secondary twins on the strengthening behaviors. However, the micro-structural deformation mechanisms of hierarchically twinned metals are still vague. For this perspective, the focus of this paper is to understand the twin spacing effects of primary/secondary twins on the flow behaviors and the related atomic-level deformation mechanisms in hierarchically twinned Cu using MD simulations.

II. SIMULATION TECHNIQUES

The MD simulations were carried out using the Large-scale Atomic/Molecular Massively Parallel Simulator (LAMMPS) code and a Cu EAM (embedded atom method) potential developed by Mishin *et al.*[30] This potential was calibrated according to the *ab initio* values of stacking faults and twin formation energies. To explore deformation mechanisms of HTS, it is necessary to simulate grains larger than those possible in fully 3-dimensional simulations. In this study, similar to the configuration used by Yamakov,[31] quasi 3-dimensional simulations with a columnar grain structure were considered. The thickness direction contains 12 atomic planes, and is along $[\bar{1}10]$. The typical relaxed nanotwinned (NT) Cu with HTS is shown in Fig. 1, with atoms colored according to common neighbor analysis (CNA) values. Gray color stands for perfect fcc atoms, red color stands for hcp atoms, and green color stands for GBs, dislocation core, free surface, and other atoms. A single line of hcp atoms represents a TB, two adjacent hcp lines stand for an intrinsic stacking fault (ISF), and two hcp lines with an fcc line between them indicates an extrinsic stacking fault (ESF). The same CNA color coding is used in the following figures. In Fig. 1(a), a polycrystalline sample with 16 grains (those without labels can be determined from periodic boundary conditions) was constructed by the Voronoi method, and the average grain size d was fixed as 70 nm (the samples have dimensions of $280 \times 280 \times 1.66\,\text{nm}^3$, and contain approximately 10 180 000 atoms). As shown in Fig. 1(b),

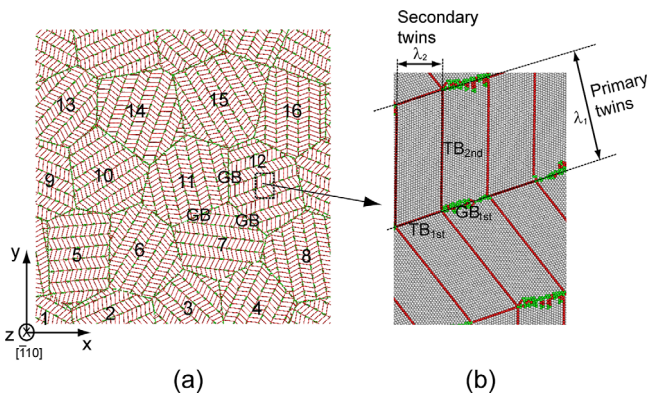

FIG. 1. (a) The relaxed NT Cu with HTS: $\lambda_1 = 10.44$ nm, $\lambda_2 = 4.17$ nm (perfect fcc atoms are not shown in this figure); (b) The corresponding amplified configurations showing the details for the primary and secondary twins.

the boundaries for the primary twins are split into TB_{1st} and GB_{1st} when the secondary twins are generated in the primary twins. The spacing for the primary twins is called λ_1, and the spacing for the secondary twins is called λ_2. The same Voronoi grain structure and the same crystallographic orientations of all grains are retained as λ_1 and λ_2 change. For $\lambda_1 = 10.44$ nm, seven samples with initial uniform secondary twins of spacing $\lambda_2 = 0.63$, 1.04, 1.67, 2.09, 3.13, 4.17, and 10.44 nm were simulated. While, for $\lambda_1 = 25.05$ nm, seven samples with initial uniform secondary twins of spacing $\lambda_2 = 0.63$, 2.09, 3.13, 4.17, 5.22, 10.44, and 20.87 nm were simulated. Periodic boundary conditions were imposed along all three directions and the tensile loading was along x direction. Before tensile loading, the as-created samples were first subjected to energy minimization by the conjugate gradient method, then gradually heated up to the desired temperature in a step-wise fashion, and finally relaxed in the Nose/Hoover isobaric-isothermal ensemble (NPT) under both the pressure 0 bar and the desired temperature (1 K) for 100 ps. After relaxation, a 20% strain was applied to each sample at a constant strain rate of $5 \times 10^8\ \text{s}^{-1}$. During the tensile loading, Nose/Hoover isobaric-isothermal ensemble (NPT) was also used, and the pressures in the y and z directions were kept to zero in order to simulate the uniaxial loading. In MD simulations, the strain rate is typically high ($>10^7$/s) and the size of system is typically small due to the inherent limitations of MD simulations. However, MD simulations have proven to be particularly useful for investigating the plastic deformation mechanism of nanocrystalline metals with carefully designed model system, in which the transient responses of the system can be examined.[32] The MD simulations should enable uncovering various deformation and microstructural processes in well-designed model systems, something that has proven difficult to achieve in experiments.

III. RESULTS AND DISCUSSIONS

In contrast to nanocrystalline metals and nanotwinned metals, hierarchically nanotwinned metals possess three characteristic microstructural length scales (the grain size d, the spacing for the primary twins λ_1, and the spacing for the secondary twins λ_2) and various boundaries, such as GBs, GB_{1st}, TB_{1st}, and TB_{2nd}. In the present study, the grain size was fixed, while the effect of spacing for primary/secondary twins on the flow behaviors was investigated. Figs. 2(a) and 2(b) show the stress-strain curves for various NT Cu samples with different λ_2 when λ_1 is 10.44 nm and 25.05 nm, respectively. Tensile stresses are observed to increase with strain up to a certain peak stress, which is associated with the onset of plastic deformation, and then gradually decrease to a steady-state value regardless of the spacing of primary/secondary twins. In order to study the change in flow stress with the spacing of primary/secondary twins, it is physically more meaningful to compare the average flow stress over a certain plastic strain interval due to the peak stress overshoot induced by the high strain rate employed in MD simulations.[6,33,34] In view of this, the average flow stress from a strain of 7%–20% is plotted against λ_2 in Fig. 2(c). For the same grain size d and the same λ_1, it can be seen from

Downloaded 13 Jun 2013 to 159.226.199.8. This article is copyrighted as indicated in the abstract. Reuse of AIP content is subject to the terms at: http://jap.aip.org/about/rights_and_permissions

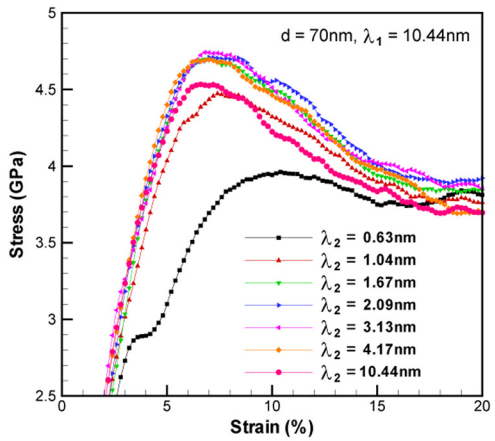

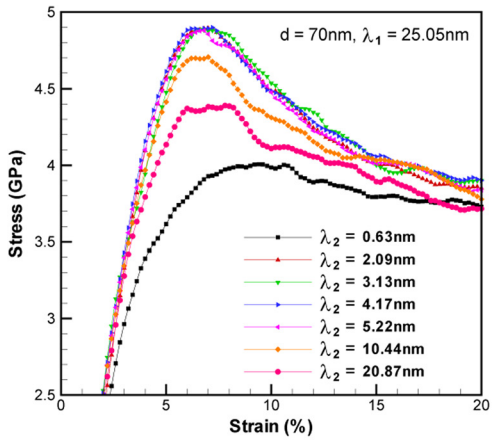

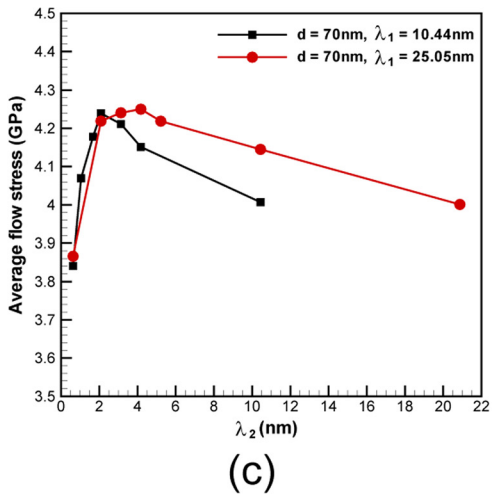

FIG. 2. Simulated stress-strain curves for the NT Cu with HTS when (a) $\lambda_1 = 10.44$ nm; (b) $\lambda_1 = 25.05$ nm; (c) The average flow stress vs. the spacing λ_2. The average flow stress was calculated from an engineering strain of 7% to 20%.

Fig. 2(c) that the average flow stress first increases as λ_2 decreases, reaching a maximum at a critical λ_2, and then decreases as λ_2 becomes even smaller. It is also observed that a higher λ_1 results in a higher critical λ_2. The critical λ_2 is around 2 nm when λ_1 is 10.44 nm, while the critical λ_2 is around 4 nm when λ_1 is 25.05 nm.

Atomic level analysis of the deformed configuration was conducted in order to understand the effect of spacing of secondary twins on the deformation mechanisms of hierarchically nanotwinned Cu. The overall simulated deformation pattern at 10% strain in the NT Cu with HTS of $\lambda_1 = 10.44$ nm and $\lambda_2 = 10.44$ nm is shown in Fig. 3(a). It should be noted that, in hierarchically nanotwinned samples containing a large number of randomly oriented grains, deformation compatibility at grain boundaries usually requires the simultaneous operations of several slip systems. As shown in the amplified configuration of Fig. 3(b) and classified by the sources of the partial dislocations, it is observed that the deformation mechanisms are dominated by the following two Hall-Petch type strengthening mechanisms when the spacing λ_2 for secondary twins is large: (1) partial dislocations emitted from GBs or GB_{1st} travel across other GBs or TBs; (2) partial dislocations emitted from TB_{1st} or TB_{2nd} travel across TB_{1st} or TB_{2nd}. In order to clearly illustrate the atomistic details for these two strengthening mechanisms, the areas A-D in Fig. 3(b) are further amplified and shown in Fig. 4. As shown in Fig. 4(a), partial dislocations are observed to nucleate from general GBs and glide along one of slip planes, finally across and intersecting with TB_{1st}, GB_{1st}, or TB_{2nd}. Partial dislocations are also observed to nucleate from GB_{1st} and leave stacking faults (ISFs or ESFs) behind, finally cut into TB_{2nd} of secondary twins, as shown in Fig. 4(b). Unlike general GBs, TBs with low excess energies usually exhibit much higher thermal and mechanical stability. So TBs can provide adequate barriers to dislocation motion for strengthening and also create more local sites for nucleating and accommodating dislocations, thereby improving ductility and work hardening.[10,35,36] However, dislocations nucleated from TBs are rarely observed by experiments and are only observed in a few cases by MD simulations.[6,37] Nanocrystalline metals with HTS possess various boundaries, such as GBs, GB_{1st}, TB_{1st}, and TB_{2nd}. The density of TB_{1st} and TB_{2nd} in nanocrystalline metals with HTS is generally high. Moreover, deformation compatibility at these TBs usually requires the simultaneous operations of several slip systems, which possibly forcing TBs to be potential nucleating sites. Here we show that TBs could provide local sites for both nucleating and accommodating dislocations. Partial dislocations are observed to nucleate from TB_{1st} of primary twins/TB_{2nd} of secondary twins, and then traveling across and intersecting with TB_{1st}/TB_{2nd}, as shown in Figs. 4(c) and 4(d), respectively. When λ_2 is large, the glide partial dislocations nucleated from GBs (including GB_{1st}) or TBs (TB_{1st} and TB_{2nd}) are blocked by other GBs or TBs, which is the main reason for strengthening.

The overall simulated deformation pattern and the corresponding amplified configuration at 10% strain in the NT Cu with HTS of $\lambda_1 = 10.44$ nm and $\lambda_2 = 0.63$ nm are shown in Figs. 5(a) and 5(b). In order to clearly illustrate the atomistic details for the deformation mechanisms, the areas A-B in Fig. 5(b) are further amplified and shown in Fig. 6. It is observed that the deformation mechanisms are dominated by the following two softening mechanisms when the spacing λ_2 for secondary twins is small: (1) partial dislocations

Downloaded 13 Jun 2013 to 159.226.199.8. This article is copyrighted as indicated in the abstract. Reuse of AIP content is subject to the terms at: http://jap.aip.org/about/rights_and_permissions

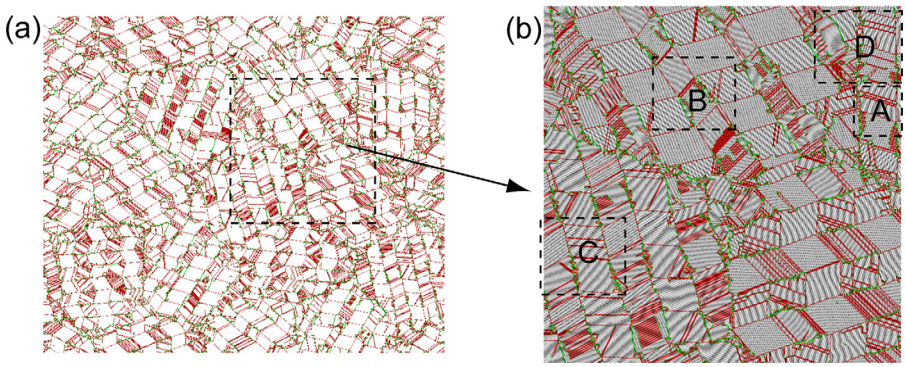

FIG. 3. (a) Simulated deformation patterns at 10% strain in the NT Cu with HTS of $\lambda_1 = 10.44$ nm, $\lambda_2 = 10.44$ nm (perfect fcc atoms are not shown in this figure); (b) The corresponding amplified configuration for the marked rectangular area in Fig. 3(a).

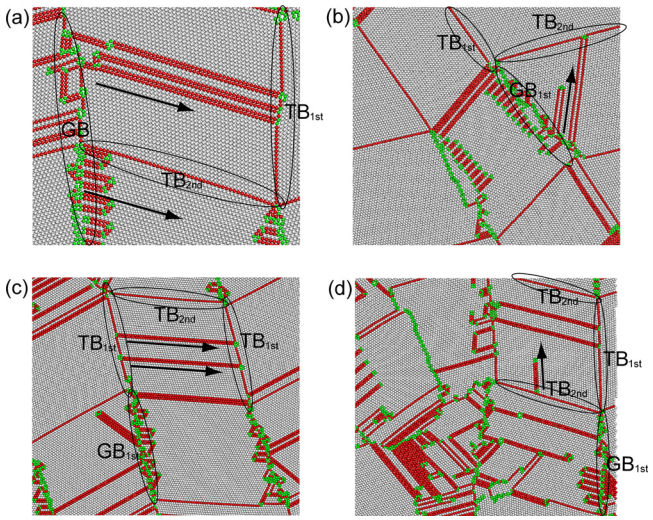

FIG. 4. The corresponding amplified configurations for the marked rectangular areas in Fig. 3(b) showing the various strengthening mechanisms: (a) partial dislocations emitted from GBs travel across TB_{1st}/GB_{1st}; (b) partial dislocations emitted from GB_{1st} travel across TB_{2nd}; (c) partial dislocations emitted from TB_{1st} travel across TB_{1st}; (d) partial dislocations emitted from TB_{2nd} travel across TB_{2nd}.

emitted from GB_{1st} or TB_{1st} travel parallel to TB_{2nd}, leading to detwinning of the secondary twins, as shown in Fig. 6(a); (2) GB_{1st} and TB_{1st} shift together, leading to thickening in one part of primary twins and thinning in the other part of primary twins, as shown in Fig. 6(b). It has been indicated that the stress required to move dislocations parallel to the TBs is on the order of 10 MPa,[6] which is negligible compared to the magnitude of stress shown in Fig. 2. Therefore, dislocations could glide easily along TBs once they are nucleated. When the detwinning is the dominating deformation mechanism, the plastic flow of NT Cu with HTS should be controlled by the nucleation rate of dislocations parallel to TBs since the critical stress to drive parallel dislocation motion is so small. Smaller λ_2 results in larger number of nucleation sources and higher nucleation rate of dislocations parallel to TBs, which giving rise to softening behaviors on the flow stress of NT Cu with HTS.

The deformation sequences showing the second softening mechanism are also shown in Fig. 7. It is observed that GB_{1st} and TB_{1st} can shift together without detwinning of the secondary twins in these regions. As suggested in the

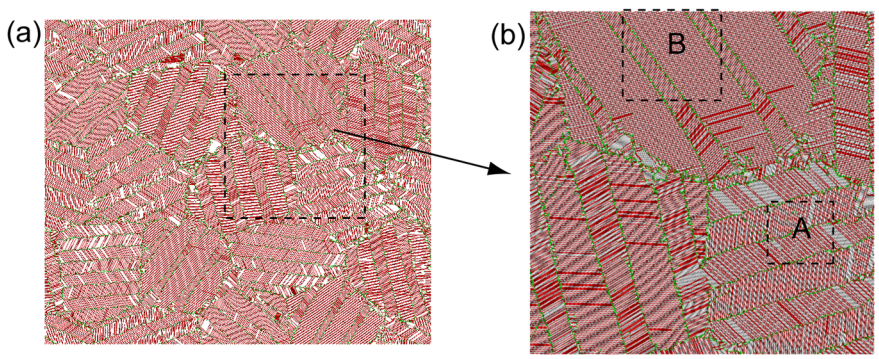

FIG. 5. (a) Simulated deformation patterns at 10% strain in the NT Cu with HTS of $\lambda_1 = 10.44$ nm, $\lambda_2 = 0.63$ nm (perfect fcc atoms are not shown in this figure); (b) The corresponding amplified configuration for the marked rectangular area in Fig. 5(a).

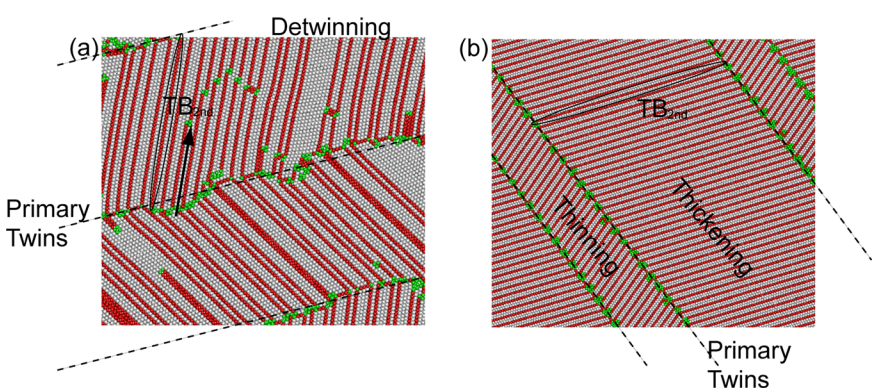

FIG. 6. The corresponding amplified configurations for the marked rectangular areas in Fig. 5(b) showing the various softening mechanisms: (a) partial dislocations emitted from GB_{1st} or TB_{1st} travel parallel to TB_{2nd}, leading to detwinning of the secondary twins; (b) GB_{1st} and TB_{1st} shift together, leading to thickening in one part of primary twins and thinning in the other part of primary twins.

Downloaded 13 Jun 2013 to 159.226.199.8. This article is copyrighted as indicated in the abstract. Reuse of AIP content is subject to the terms at: http://jap.aip.org/about/rights_and_permissions

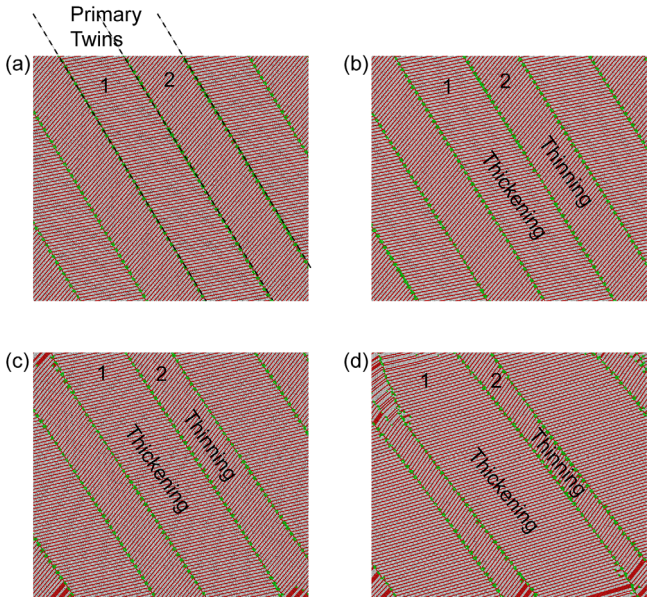

FIG. 7. The amplified deformation sequences showing the second softening mechanism in the NT Cu with HTS of $\lambda_1 = 10.44$ nm, $\lambda_2 = 0.63$ nm: (a) at strain of 2%; (b) at strain of 3%; (c) at strain of 5%; (d) at strain of 10%.

previous research,[6,10,35] the glide of twinning partials on TBs mediates the TB migration, giving rise to the deformation-induced detwinning that leads to softening behaviors. However, the second softening behavior observed here is a new deformation mechanism for hierarchically nanotwinned metals, and should also contribute to the observed decreasing trend of flow strength with decreasing λ_2 when λ_2 is below the critical spacing. For the nanocrystalline metals without NT structures, MD simulations have shown a transition from dislocation-mediated plastic deformation to GB-associated mechanisms such as GB sliding, GB diffusion, and grain rotation when the grain size is reduced to below 10 nm in Cu.[33] The softened behaviors below 10 nm is mainly due to the GB-associated mechanisms. The boundaries for the primary twins are split into TB_{1st} and GB_{1st} when the secondary twins are generated in the primary twins. So the shifting and diffusion of the boundaries of primary twins should also contribute to the observed softening behaviors for similar reason. As suggested in the present study, there exists a transition in dominating deformation mechanisms, occurring at a critical spacing of λ_2 for which strength is maximized. Above the critical spacing of λ_2, the deformation mechanisms are dominated by the two Hall-Petch type strengthening mechanisms. While below the critical spacing of λ_2, the deformation mechanism is dominated by the two softening mechanisms.

IV. SUMMARY

In the present study, a series of large-scale molecular dynamics simulations have been performed to investigate the deformation mechanisms of hierarchically nanotwinned Cu. For the same grain size d and the same spacing of primary twins λ_1, the average flow stress first increases with the decreasing spacing of secondary twins λ_2, reaching a maximum at a critical λ_2, and then drops as λ_2 becomes even smaller. The smaller the spacing for λ_1, the smaller the critical spacing for λ_2. There exists a transition in dominating deformation mechanisms, occurring at a critical spacing of λ_2 for which strength is maximized. Above the critical spacing of λ_2, the deformation mechanisms are dominated by the two Hall-Petch type strengthening mechanisms: (1) partial dislocations emitted from GBs travel across other GBs or TBs; (2) partial dislocations emitted from TB_s travel across other TB_s. However, the deformation mechanism are dominated by the two softening mechanisms below the critical spacing of λ_2: (1) partial dislocations emitted from boundaries of primary twins travel parallel to TB_{2nd}, leading to detwinning of the secondary twins; (2) boundaries of primary twins shift together, leading to thickening in one part of primary twins and thinning in the other part of primary twins. The results in the present paper will provide insights for achieving higher strength in the hierarchically nanotwinned metals by controlling the twin spacing of primary/secondary twins.

ACKNOWLEDGMENTS

The authors would like to acknowledge the financial support of the National Key Basic Research Program of China (Grants Nos. 2012CB932203 and 2012CB937500) and NSFC (Grants Nos. 11002151, 11222224, 11072243, and 11021262). The simulations reported were performed at Supercomputing Center of Chinese Academy of Sciences.

[1]M. A. Meyers, A. Mishra, and D. J. Benson, Prog. Mater. Sci. **51**, 427 (2006).
[2]M. Dao, L. Lu, R. J. Asaro, J. T. M. De Hosson, and E. Ma, Acta Mater. **55**, 4041 (2007).
[3]L. Lu, Y. Shen, X. Chen, L. Qian, and K. Lu, Science **304**, 422 (2004).
[4]L. Lu, X. Chen, X. Huang, and K. Lu, Science **323**, 607 (2009).
[5]Y. F. Shen, L. Lu, M. Dao, and S. Suresh, Scr. Mater. **55**, 319 (2006).
[6]X. Y. Li, Y. J. Wei, L. Lu, K. Lu, and H. J. Gao, Nature **464**, 877 (2010).
[7]Y. J. Wei, Phys. Rev. B **83**, 132104 (2011).
[8]F. P. Yuan and X. L. Wu, Phys. Rev. B **86**, 134108 (2012).
[9]L. L. Zhu, H. H. Ruan, X. Y. Li, M. Dao, H. J. Gao, and J. Lu, Acta Mater. **59**, 5544 (2011).
[10]Y. T. Zhu, X. Z. Liao, and X. L. Wu, Prog. Mater. Sci. **57**, 1 (2012).
[11]N. Hansen, Metall. Mater. Trans. A **32**, 2917 (2001).
[12]B. Bay, N. Hansen, D. A. Hughes, and D. Kuhlmann, Acta Metall. Mater. **40**, 205 (1992).
[13]R. Z. Valiev, R. K. Islamgaliev, and I. V. Alexandrov, Prog. Mater. Sci. **45**, 103 (2000).
[14]Y. Iwahashi, Z. Horita, M. Nemoto, and T. G. Langdon, Acta Mater. **46**, 3317 (1998).
[15]T. Hebesberger, H. P. Stüwe, A. Vorhauer, F. Wetscher, and R. Pippan, Acta Mater. **53**, 393 (2005).
[16]Y. S. Li, Y. Zhang, N. R. Tao, and K. Lu, Scr. Mater. **59**, 475 (2008).
[17]Y. S. Li, N. R. Tao, and K. Lu, Acta Mater. **56**, 230 (2008).
[18]K. Lu and J. Lu, Mater. Sci. Eng. A **375–377**, 38 (2004).
[19]K. Wang, N. R. Tao, G. Liu, J. Lu, and K. Lu, Acta Mater. **54**, 5281 (2006).
[20]T. H. Fang, W. L. Li, N. R. Tao, and K. Lu, Science **331**, 1587 (2011).
[21]H. N. Kou, Ph.D. dissertation, The Hong Kong Polytechnic University, 2011.
[22]N. R. Tao and K. Lu, Scr. Mater. **60**, 1039 (2009).
[23]Y. T. Zhu, J. Narayan, J. P. Hirth, S. Mahajan, X. L. Wu, and X. Z. Liao, Acta Mater. **57**, 3763 (2009).
[24]A. J. Cao and Y. G. Wei, Appl. Phys Lett. **89**, 041919 (2006).
[25]J. Narayan and Y. T. Zhu, Appl. Phys. Lett. **92**, 151908 (2008).
[26]X. L. Wu, J. Narayan, and Y. T. Zhu, Appl. Phys. Lett. **93**, 031910 (2008).
[27]S. A. Dregia and J. P. Hirth, J. Appl. Phys. **69**, 2169 (1991).
[28]C. H. Henager, Jr. and R. G. Hoagland, Scr. Mater. **50**, 701 (2004).
[29]L. L. Zhu, H. N. Kou, and J. Lu, Appl. Phys Lett. **101**, 081906 (2012).

Downloaded 13 Jun 2013 to 159.226.199.8. This article is copyrighted as indicated in the abstract. Reuse of AIP content is subject to the terms at: http://jap.aip.org/about/rights_and_permissions

[30]Y. Mishin, M. J. Mehl, D. A. Papaconstantopoulos, A. F. Voter, and J. D. Kress, Phys. Rev. B **63**, 224106 (2001).
[31]V. Yamakov, D. Wolf, S. R. Phillpot, A. K. Mukherjee, and H. Gleiter, Nature Mater. **1**, 45 (2002).
[32]D. Wolf, V. Yamakov, S. R. Phillpot, A. K. Mukherjee, and H. Gleiter, Acta Mater. **53**, 1 (2005).
[33]J. Schiotz and K. W. Jacobsen, Science **301**, 1357 (2003).
[34]J. B. Jeon, B. Lee, and Y. W. Chang, Scr. Mater. **64**, 494 (2011).
[35]T. Zhu and H. J. Gao, Scr. Mater. **66**, 843 (2012).
[36]K. Lu, L. Lu, and S. Suresh, Science **324**, 349 (2009).
[37]Z. S. You, X. Y. Li, L. J. Gui, Q. H. Lu, T. Zhu, H. J. Gao, and L. Lu, Acta Mater. **61**, 217 (2013).

Downloaded 13 Jun 2013 to 159.226.199.8. This article is copyrighted as indicated in the abstract. Reuse of AIP content is subject to the terms at: http://jap.aip.org/about/rights_and_permissions